



# Impact of Cumulus Microphysics and Entrainment Specification on Tropical Cloud and Radiation in GFDL AM2

Yanluan Lin<sup>1</sup>

Received: 25 March 2019 / Accepted: 6 May 2019 / Published online: 15 May 2019  
© King Abdulaziz University and Springer Nature Switzerland AG 2019

## Abstract

Clouds and precipitation simulated by climate models still have a large room for improvement. Geophysical Fluid Dynamics Laboratory (GFDL) High-Resolution Atmospheric Model (HiRAM) has much larger ice water path (IWP, ~ 5 times) and stratiform precipitation fraction (~ 10 times) than its Atmospheric Model version 2 (AM2) over the Tropics. It is found that such differences are mainly due to the replacement of the relaxed Arakawa Schubert (RAS) scheme in AM2 by the modified University of Washington (UW) shallow convection used in HiRAM. The focus of the study is to investigate the sensitivity of simulated cloud, precipitation, and radiation to the two key parameters (precipitation efficiency and entrainment specification) in RAS, and interpret the difference between AM2 and HiRAM. With more deep plumes inhibited, the convective heating and moistening decrease, and the upper troposphere becomes colder and drier. With reduced precipitation efficiency, more convective condensate is detrained and stratiform precipitation increases. Both precipitation efficiency and entrainment specification change the vertical heating profiles and precipitation partitioning, but via different mechanisms. Using offline radiation calculations, convection scheme-induced tropical radiation variation is investigated. Increased longwave trapping by increased upper level ice clouds is partially compensated by a dry and cold bias in the upper troposphere. However, top of atmosphere absorbed shortwave reduction is proportional to increased IWP, but the reduction is not as large as that computed using offline radiation calculation assuming similar increase of IWP. The reason is that the increased IWP associated with large-scale precipitation does not peak around noon with the maximum solar radiation as that associated with convective precipitation. The study highlights the importance of convective parameterization in regulating tropical clouds and radiation.

**Keywords** Convective parameterization · Cloud · Radiation · Entrainment

## 1 Introduction

Clouds simulated by general circulation models (GCMs) vary significantly in terms of cloud properties, such as ice water content, liquid water content, and cloud cover (Waliser et al. 2009; Li et al. 2012; Klein et al. 2013), which are strongly impacted by model cloud microphysics and macrophysics schemes. However, the impacts of convection scheme on model simulated clouds are subtle and indirect. Due to the close interactions and relationships between convection schemes and cloud schemes in current GCMs, convection schemes also have significant impacts on model

cloud simulations (e.g., Lin et al. 2012, 2013; Zhao 2014; Zhao et al. 2016). Convection scheme can directly impact model clouds via detrainment, a source of cloud condensate to the large-scale cloud schemes (Park et al. 2014; Donner et al. 2011). Another pathway for the convection scheme to impact model clouds is via the control of the occurrence frequency and intensity of convection. This pathway is indirect and mostly related to the partitioning of model precipitation between convective and large-scale components (Lin et al. 2013). However, this connection has not been systematically studied and well documented.

Precipitation, clouds, and radiation have distinct characteristics closely related to convection in the Tropics (Elsaesser et al. 2010; Kubar and Hartmann 2008; Kikuchi and Wang 2008; Ehsan et al. 2017a, b; among others). As a result, convection representation in GCMs has a strong impact on model cloud and precipitation simulations over the tropics (e.g., Lin et al. 2013). However, such impacts,

✉ Yanluan Lin  
yanluan@tsinghua.edu.cn

<sup>1</sup> Ministry of Education Key Laboratory for Earth System Modeling, Department of Earth System Science, Tsinghua University, Beijing 100084, China

sometimes, are not explicitly emphasized in relevant cloud evaluation studies (Waliser et al. 2009), because model clouds are generally not directly related with convection schemes. Instead, model clouds are closely related to large-scale cloud schemes, including the microphysics and macrophysics in the model. Studies investigating the impacts of cloud schemes on model clouds are widespread. For example, ubiquitous underestimate of middle clouds (Zhang et al. 2005), up to two orders of magnitude different ice water path (Waliser et al. 2009), and others have been noted. In contrast, there are few papers focused on the impacts of convection schemes on model simulated clouds (Clement and Soden 2005; Held et al. 2007; Lin et al. 2013).

Cumulus entrainment (Arakawa 2004; de Rooy and Siebesma 2010) and cumulus microphysics (e.g., Emanuel and Zivkovic-Rothman 1999; Del Genio et al. 2005; Song and Zhang 2011) remain the two most uncertain parts of convective parameterizations. Both strongly impact GCM performance and their climate sensitivity (Del Genio et al. 2005; Bechtold et al. 2008; Sanderson et al. 2008; Zhao 2014). Cumulus parameterizations generally include a simple representation of microphysics (Donner et al. 2001; Del Genio et al. 2005; Zhao et al. 2009) or use an empirical precipitation efficiency (PE) to simplify the complex cumulus precipitation processes. With detrained condensate treated as a source for large-scale condensate following Tiedtke (1993) in GFDL AM2 (Anderson et al. 2004), PE impacts the partitioning of convective condensate between precipitating particles and detrained condensate and, thus, the convective and stratiform precipitation partitioning. Various entrainment parameterizations, from a simple relationship between entrainment rate and cloud radius (Simpson and Wiggert 1969) or plume depth (Moorthi and Suarez 1992) to environment-dependent specifications (Bechtold et al. 2008; Chikira and Sugiyama 2010), have been applied in various mass flux schemes (de Rooy and Pier Siebesma 2010 and references therein). By applying an entrainment limiter to prevent deep plumes from occurring, Tokioka et al. (1988) found model simulations of tropical transient circulations were strongly impacted. Held et al. (2007) found that cloud condensate and stratiform precipitation fraction vary with this entrainment limiter in the relaxed Arakawa–Schubert (RAS, Moorthi and Suarez 1992) scheme using an idealized model setting, as do the cloud radiative forcing and total condensed water path. This suggests a significant impact of cumulus parameterization on cloud simulations. However, how cumulus parameterization impacts model cloud and precipitation has not been intensively analyzed.

The previous studies have emphasized the impact of cloud schemes on cloud simulations (Fowler et al. 1996; Webb et al. 2001; Shimpo et al. 2008), but, here, we focus on convection scheme. With detrainment from deep convection and the interaction between large-scale clouds with convective

updrafts included in GCMs (Tiedtke 1993; Fowler and Randall 2002; Anderson et al. 2004), cumulus parameterizations also impact cloud simulations. As a first step, we compare tropical clouds and precipitation between Geophysical Fluid Dynamics Laboratory (GFDL) AM2 and High-Resolution AM2 (HiRAM, Zhao et al. 2009) and explore how convection schemes modulate model cloud, precipitation, and radiative properties. A series of sensitivity experiments via change of PE and entrainment limiter in RAS are used to investigate their impacts on model cloud simulations. We further explore how these two key parameters impact top of atmosphere (TOA) radiation using a set of offline radiation calculations. We focus on the Tropics, since tropical cloud and precipitation are dominated by convection.

The paper is organized as follows: data and model experiments are introduced in Sect. 2. How precipitation efficiency and entrainment specification impact tropical clouds and radiation is explored in Sect. 3. Section 4 introduced the offline radiation calculations and their analysis. A brief summary and discussion of the study is included in Sect. 5.

## 2 Data and Model Experiments

Since its operation in June 2006, the cloud profiling radar on the CloudSat satellite has collected vertical profiles of radar reflectivity factor. Retrievals of ice water content (IWC) based on radar reflectivity and temperature has been released and used for model evaluation (Waliser et al. 2009; Li et al. 2012). The minimum detectable IWC is estimated to be approximately  $5 \text{ mg m}^{-3}$  and the retrieved IWC includes the contributions from snow and graupel owing to the strong dependence of radar reflectivity on particle sizes.

Tropical Rainfall Measuring Mission (TRMM) rainfall product (3G68, Kummerow et al. 2001) provides precipitation rates and convective precipitation fraction at 1-h resolution and  $0.5^\circ \times 0.5^\circ$  over the Tropics (40S–40N) from passive microwave and precipitation radar sensors. Precipitation climatology from 12 years (1998–2009) is used for the convective precipitation fraction and precipitation diurnal cycle estimates. The data are interpolated to the same resolution as model ( $2.5^\circ \times 2.0^\circ$ ) for comparison. We also use the Global Precipitation Climatology Project (GPCP) version 2 data sets (Adler et al. 2003) for precipitation comparison. Longwave and shortwave radiation from CERES-EBAF (Cloud and the Earth's Radiant Energy System Energy Balanced and Filled, Loeb et al. 2009) was used.

Based on GFDL AM2, a high-resolution AM2 (HiRAM) well able to simulate tropical cyclones was developed (Zhao et al. 2009). The major change from AM2 to HiRAM (Table 1) is the replacement of RAS by UW shallow convection scheme (Zhao et al. 2009). RAS uses a spectrum of entraining plumes with a closure that relaxes the cloud work

**Table 1** A brief summary of differences between AM2 and HiRAM

	AM2	HiRAM
Resolution	2°×2.5°, latitude–longitude grid	~0.5°, cubed sphere
Convection scheme	RAS	Modified UW
Cloud fraction scheme	Tiedtke (1993)	A simple diagnostic scheme
Vertical levels	24	32
Radiation	Slingo (1989) and Fu and Liou (1993)	Slingo (1989) and Fu and Liou (1993)

Refer to the text for more details

function back to a critical value over a time scale varying from 2 h for shallow convection to 12 h for deep convection. It separates updrafts detraining above 500 hPa and below 800 hPa as deep and shallow convection, respectively (Anderson et al. 2004). Precipitation efficiency (PE), defined as the fraction of water condensed in the cumulus updrafts that becomes precipitation, is a constant (0.975 for deep and 0.5 for shallow convection) in the standard AM2. Entrainment rate is inversely proportional to the plume depth in RAS, and a Tokioka limiter (Tokioka et al. 1988) is used to inhibit the deep (weakly entraining) plumes in AM2. Assuming a subcloud layer depth of 1 km, a Tokioka limiter constant of 0.025 used in standard AM2 gives an equivalent fractional entrainment rate of 0.025 km<sup>-1</sup>. In comparison, UW uses a single plume with entraining and detraining profiles determined by a parcel buoyancy sorting algorithm with a plume vertical momentum equation (Bretherton et al. 2004). The plume base mass flux is determined by the boundary layer turbulence kinetic energy and convective inhibition. The scheme also includes a cloud top penetrative entrainment and a simple cloud microphysics with a temperature-dependent autoconversion threshold. Note that the upper limit of the vertical extent of the convective clouds assumed in the original UW was removed in HiRAM to allow for deep convection occurrence. It is assumed that the entrainment rate scales inversely with cumulus height and the scale ( $c_0$  in Eq. 18 of Bretherton et al. 2004) is ten over ocean and reduced by half over land for low-resolution simulations (Zhao et al. 2009). Note that the value of  $c_0$  over land has a strong impact on precipitation over tropical land areas, including its peak in the mid-afternoon. Assuming a convection height of 10 km, fractional entrainment rate in UW is 1 km<sup>-1</sup> over ocean and 0.5 km<sup>-1</sup> over land. This is more than one order of magnitude larger than that in AM2. For the convective precipitation, a simple autoconversion parameterization assuming a symmetric triangle distribution of total condensate with a fixed width of 0.5 g kg<sup>-1</sup> and a threshold value of 1 g kg<sup>-1</sup> was used in UW. In summary, two major differences between RAS and UW are PE and entrainment specification.

There are a few other changes (Table 1) between AM2 and HiRAM, such as using the latitude–longitude–grid (2° latitude×2.5° longitude) in AM2 to the cubed sphere

(~0.5°) in HiRAM and vertical levels increased from 24 in AM2 to 32 in HiRAM, (Zhao et al. 2009). The prognostic cloud fraction scheme (Tiedtke 1993) in AM2 was also replaced by a relatively simple diagnostic scheme assuming a subgrid-scale distribution of total water (Zhao et al. 2009). However, most of the noted change in clouds and precipitation is dominated by the replacement of RAS by the UW scheme as noted below.

To investigate the impact of PE and entrainment specification on tropical cloud and precipitation, a series of RAS sensitivity simulations using varying PE (0.9, 0.8, 0.7, and 0.6) and Tokioka (TK) limiter constant (0.05, 0.1, and 0.2) for deep convection are conducted (Table 2). Another experiment, identical to AM2, except with RAS replaced by UW (hereafter called as AM2-UW) is also conducted for comparison. All the experiments in Table 2 are 5 year 2-degree AMIP-type simulations based on AM2 using prescribed climatology of SST and sea ice except HiRAM, which has a resolution of ~50 km. Note that the inclusion of HiRAM here is mainly to motivate the study, while the focus of the

**Table 2** Description of the experiments used in the study

Experiment	Model	Convective scheme	PE parameter value	TK parameter value
AM2	AM2	RAS	0.975	0.025
HiRAM	HiRAM	UW		
AM2-UW	AM2	UW		
RAS-PE6	AM2	RAS	0.6	0.025
RAS-PE7	AM2	RAS	0.7	0.025
RAS-PE8	AM2	RAS	0.8	0.025
RAS-PE9	AM2	RAS	0.9	0.025
RAS-TK2	AM2	RAS	0.975	0.05
RAS-TK4	AM2	RAS	0.975	0.1
RAS-TK8	AM2	RAS	0.975	0.2

Refer to the text for more details

RAS is relaxed Arakawa Schubert scheme (Moorthi and Suarez 1992) used in AM2; UW is the modified University of Washington shallow convection scheme (Bretherton et al. 2004) used in HiRAM (Zhao et al. 2009)

PE precipitation efficiency for deep convection, TK Tokioka limiter constant in RAS

study is on the sensitivity of simulated cloud, precipitation, and radiation in AM2 to the two key parameters in RAS. As PE decreases, more convective condensate is detrained to become stratiform condensate instead of being removed directly as surface precipitation. As Tokioka limiter constant increases, plumes with smaller entrainment rate (i.e., deep plumes) are prevented from occurring, especially in a dry environment. Note that this is different from UW, which has one plume and uses a larger entrainment rate to constrain convection height and intensity. Cloud radiation calculation is identical for these simulations with liquid cloud radiative properties from Slingo (1989) and ice clouds following Fu and Liou (1993).

### 3 Results

Although the mean climate, including precipitation, and TOA radiation balance (Anderson et al. 2004, Zhao et al. 2009) are similar in AM2 and HiRAM, their ice water content (IWC) and ice water path (IWP) differ significantly (Figs. 1, 2). HiRAM has much larger IWC ( $\sim 10 \text{ mg m}^{-3}$ ) than AM2 ( $\sim 2 \text{ mg m}^{-3}$ ) over the tropical upper troposphere and is close to CloudSat retrievals (Waliser et al. 2009, Fig. 1). IWC maximizes around 300 hPa in AM2, while it

is near 500 hPa in HiRAM over the Tropics. Note that IWC and IWP in the models include ice and snow, since ice falling out of a cloud layer is a source of ice for the layer below (Rotstajn 1997). Similarly, HiRAM has  $\sim 5$  times larger zonal mean IWP than AM2 over the Tropics with a relatively small ( $\sim 20$  to  $30\%$ ) increase of IWP over the mid- and high-latitudes (Fig. 2a).

Zonal mean total precipitation is comparable among GPCP (Huffman et al. 2007), AM2, and HiRAM, with slightly reduced precipitation south of the Equator and increased precipitation over the NH and SH storm tracks for HiRAM (Fig. 2b). However, HiRAM has much larger stratiform precipitation than AM2, especially over the Tropics (Fig. 2b). Overall, HiRAM has much larger IWP and stratiform precipitation fraction (SPF) than AM2, especially over the Tropics. Note that the above noted differences between AM2 and HiRAM are also manifested between AM2 and AM2\_UW. For example, IWC, IWP, and stratiform precipitation are close to each other between AM2\_UW and HiRAM (Figs. 1, 2). This suggests that cloud and precipitation changes from AM2 to HiRAM are mainly related to the replacement of RAS by the UW scheme, since it is the only difference between AM2 and AM2\_UW (Table 1).

Although the definition of stratiform precipitation differs in observations and models, stratiform precipitation

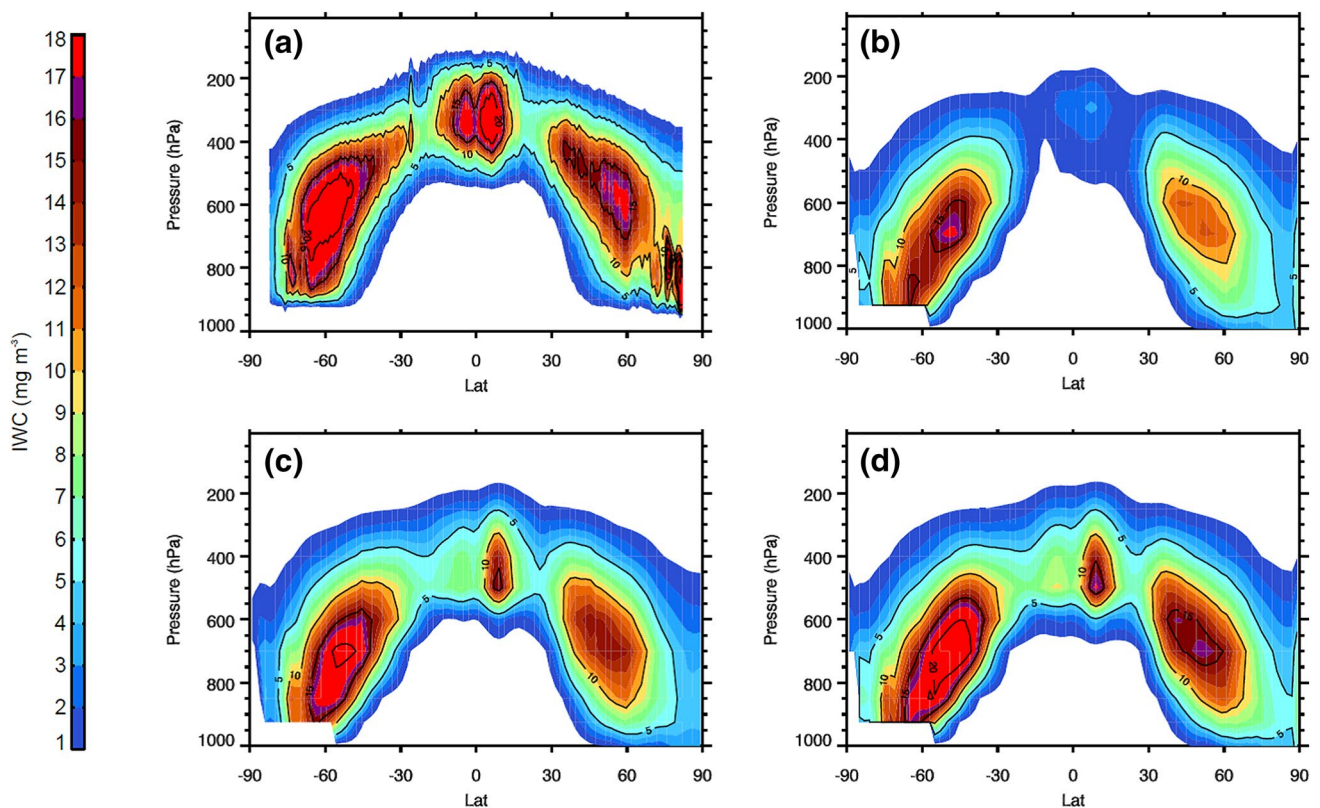


**Fig. 1** Latitude–pressure plot of zonal mean ice water content from **a** CloudSat retrievals, **b** AM2, and **c** HiRAM, and **d** AM2-UW

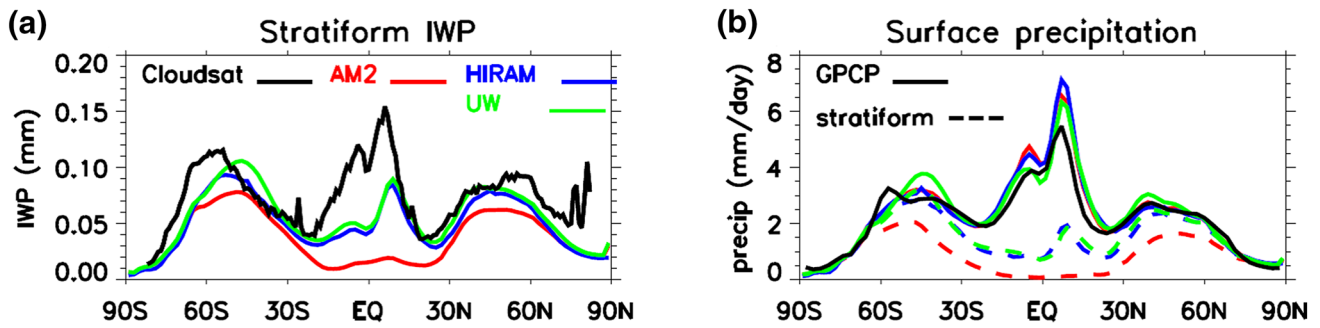
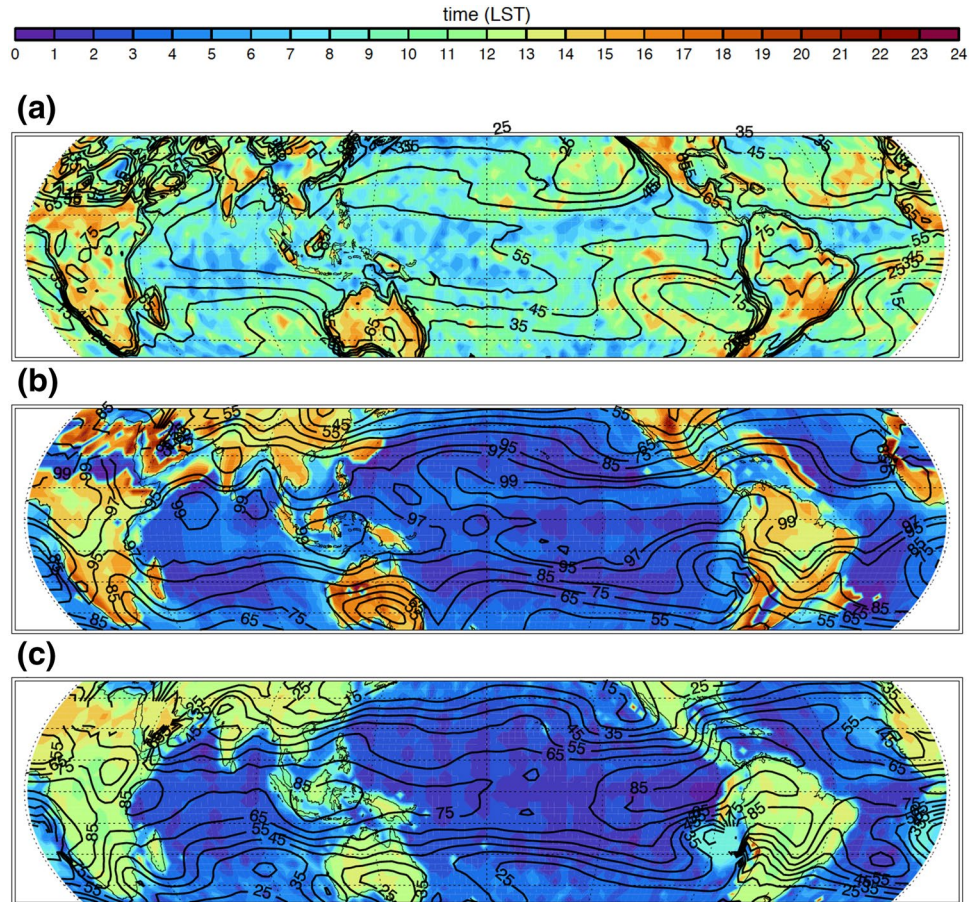


**Fig. 2** Zonal mean model results compared with available observations for **a** IWP and **b** precipitation. Dashed lines in **b** denote the stratiform precipitation of the model simulations. GPCP is Global Precipitation Climatology Project version 2 data sets (Adler et al. 2003)

fraction over the tropics in HiRAM is close to TRMM estimates (Fig. 3). Convective precipitation only contributes to 50–60% and 75–80% of total precipitation over the tropical ocean and land area in TRMM retrievals (Fig. 3a), but the contribution is over 95% in the tropics in AM2 (Fig. 3b). In contrast, this value is reduced to ~75% in HiRAM (Fig. 3c) and becomes much closer to the TRMM estimate. This ameliorates a general underestimate of stratiform precipitation in the tropics by climate models as emphasized before (e.g., Dai 2006). Similar to previous studies (e.g., Yang and Slingo

2001), rainfall peaks in the late afternoon over land and in the early morning over the deep tropics in TRMM retrievals (Fig. 3a). Although both AM2 and HiRAM capture the different rainfall peaks over land and ocean, the peak time over land is a few hours delayed in AM2. This is due to the 12-h relaxation time used in RAS. Reduced relaxation time generally leads to increased convective precipitation with a slightly earlier peak over land, and vice versa. Instead, rainfall peak at noon following the maximum solar radiation in HiRAM is mainly due to the small  $c_0$  as mentioned

**Fig. 3** Convective precipitation percentage (contours) and local standard time (LST) of the maximum precipitation (color shading) from **a** TRMM, **b** AM2, and **c** HiRAM





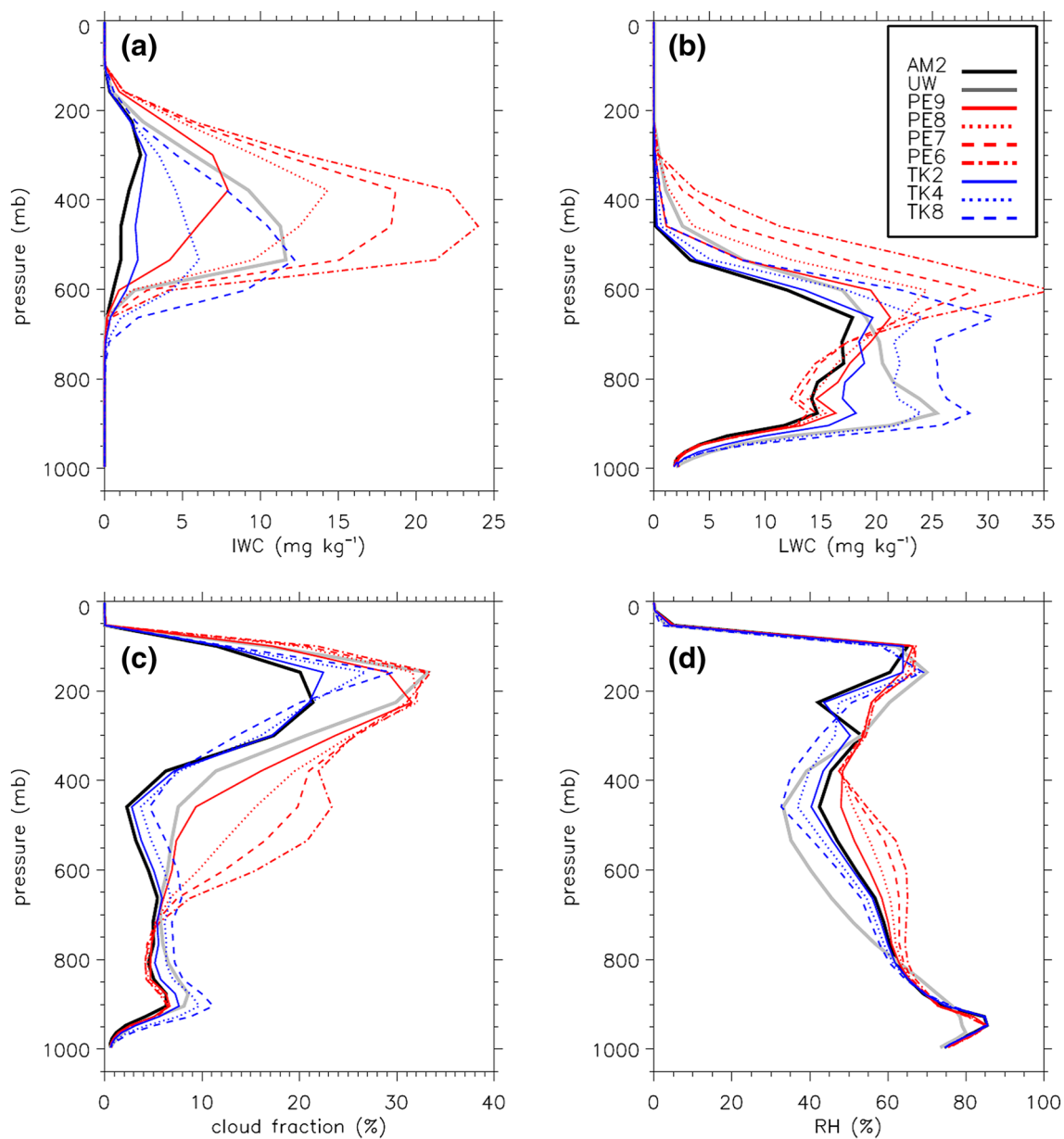


**Fig. 5** Tropical mean profiles of **a** IWC, **b** LWC, **c** cloud fraction, and **d** relative humidity for various AM2 sensitivity experiments

in RAS-PE simulations mainly results directly from the increased detrainment from convection with a minor increase from the increased large-scale condensation.

For TK, the picture is different. Without the direct increased source of condensate from convective detrainment, the increase of condensate in RAS-TK runs is smaller than RAS-PE runs and mostly results from the increase of stratiform precipitation. As deep convective plumes are inhibited with increased TK limiter constant, convective heating is reduced accordingly, especially in the upper troposphere (Fig. 7a). Large-scale condensation strives to maintain the magnitude of the total heating, but it cannot easily reach

above 400 hPa probably due to the strong grid-scale vertical motion required for the large-scale condensation (Fig. 7b). Tropical upper troposphere heating is mainly achieved by the stratiform heating associated with mesoscale convective complex in nature (Houze 2004), but this process is not directly considered in the model. UW has the maximum stratiform heating near 400 hPa, which is also slightly lower than the convective heating in AM2. It appears that the stratiform heating cannot reach as high as the convective heating in both RAS-TK and AM2-UW runs. As a result, the sum of convective and large-scale heating becomes smaller in the upper troposphere, with a  $0.8 \text{ K day}^{-1}$  decrease from AM2

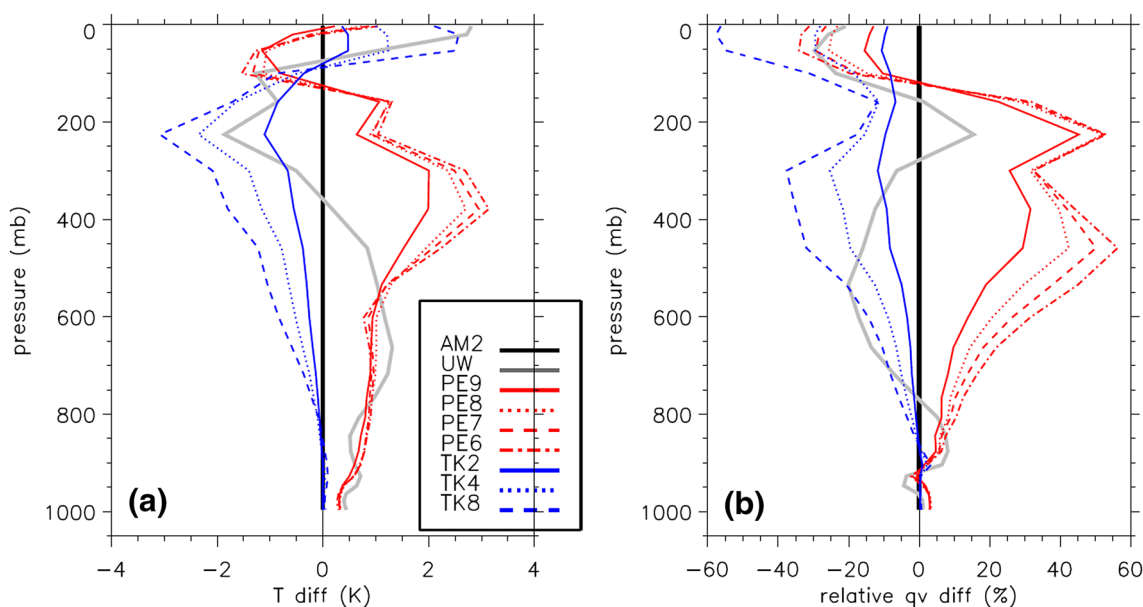


**Fig. 6** Tropical mean profiles of various AM2 sensitivity experiments relative to AM2 for **a** temperature and **b** relative specific humidity

to RAS-TK8 and AM2-UW (Fig. 7d). It is worth to note that convective and large-scale heating rates compensate, so that total heating is more or less the same regardless of parameter or scheme. The main reason is that the atmosphere over the tropics is in quasi-equilibrium from a balance between the diabatic heating and longwave cooling. These simulations have approximately the same total precipitation, since it is mainly controlled by the radiative cooling of the atmosphere (e.g., Lin et al. 2013). Convection scheme mainly regulates the partitioning of precipitation, but not the total precipitation. The radiative heating from TK runs only differs slightly from AM2 compared with PE runs (Fig. 7c). For example, with the huge change of clouds, longwave cooling is reduced by  $\sim 0.8 \text{ K day}^{-1}$  with a shortwave heating reduction of only  $0.1 \text{ K day}^{-1}$  below 600 hPa for RAS-PE6 (Fig. 7c). As a result, it is colder in the upper troposphere in RAS-TK8 and AM2-UW (Fig. 6a). Both PE and TK runs also change the temperature and moisture profiles. The middle and upper troposphere (below 150 hPa) is warmer and moister in RAS-PE runs but colder and drier in RAS-TK runs. Above 100 hPa, reduced RAS-PE runs are colder and drier, but RAS-TK runs are warmer and drier (Fig. 6).

In all these comparisons, we note that AM2-UW is generally similar to RAS-TK runs in terms of cloud fraction and IWC, especially to RAS-TK8. For example, AM2-UW has similar IWP (Fig. 4a), IWC (Fig. 5a), and convective and large-scale heating (Fig. 7a, b) as RAS-TK8. Convective heating rates decrease quickly to near zero around 300 hPa in AM2-UW (Fig. 7a). This is because plumes in UW entrain more and reach lower levels more frequently than those in RAS. To maintain a near moist adiabatic profile over the

Tropics, large-scale condensation becomes more active in UW to partially compensate for the inefficient convective heating above 600 hPa. As a result, AM2-UW and RAS-TK8 have a heating structure featuring a large-scale condensational heating in the upper troposphere and an evaporative cooling in the lower troposphere. Such a heating pattern is known to be important for many convective systems, such as Kelvin waves and Madden–Julian Oscillation (Lin et al. 2004; Kiladis et al. 2009). In contrast, large-scale evaporation dominates below 300 hPa in AM2. Both the larger SPF and increased stratiform condensation heating in the upper troposphere in AM2-UW and RAS-TK8 are consistent with observational studies as summarized in Houze (2004) and Kiladis et al. (2009). The main reason for this is the larger master entrainment rate used in UW and the increased entrainment limiter constant used in RAS-TK8.

#### 4 Offline Radiation Calculations

Clouds significantly influence both longwave and shortwave radiative fluxes. However, other atmospheric properties, such as moisture and temperature, also impact radiation. For shortwave, diurnal variation of clouds also matters. Not only cloud properties change in these sensitivity simulations, but temperature and moisture profiles also differ. As a result, radiation differences among these simulations are a result of a combination of differing factors. To isolate radiative impacts by clouds from other factors, we use offline radiation calculations. These calculations also serve to see how

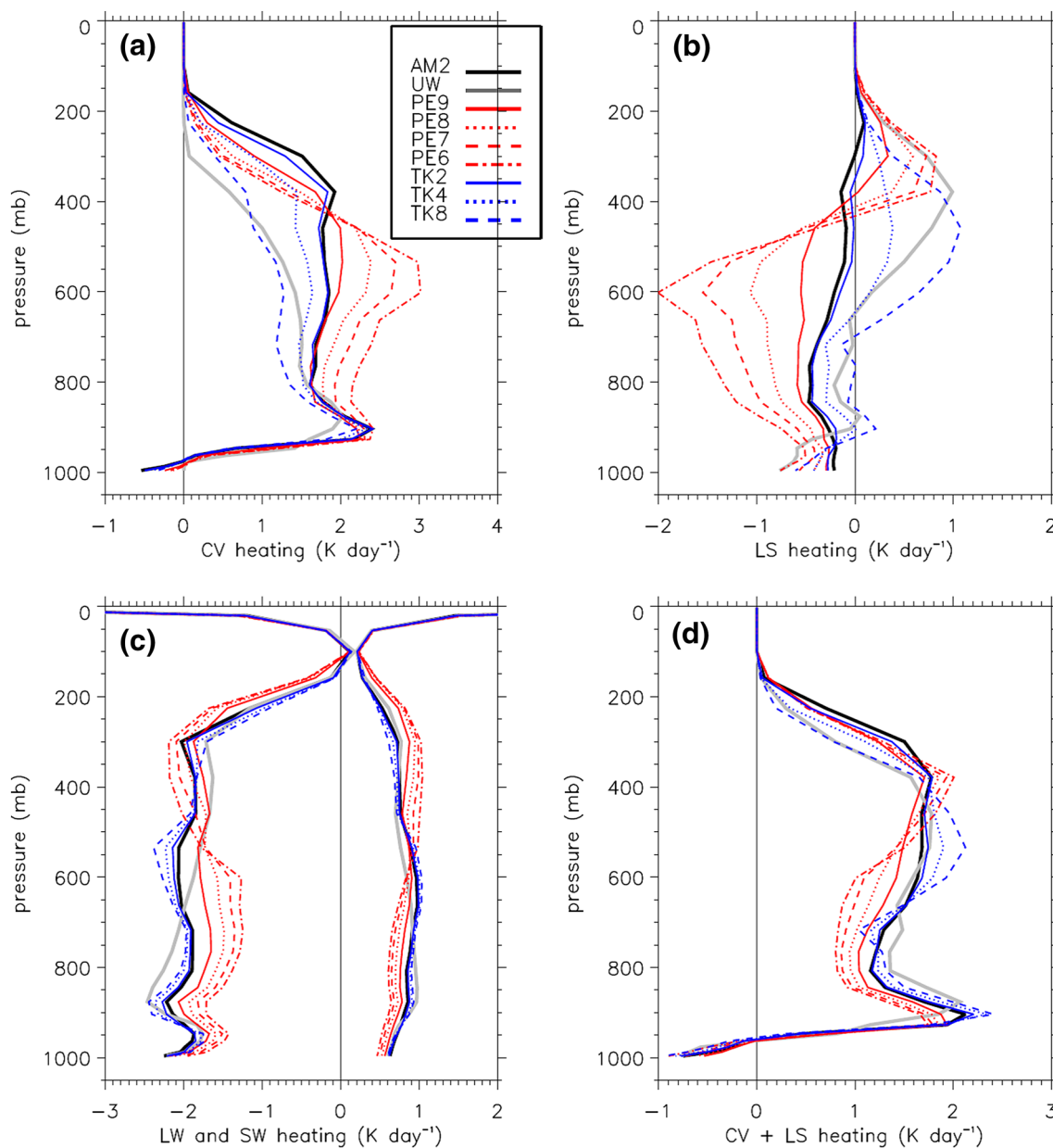


**Fig. 7** Tropical mean profiles of **a** convective heating rates, **b** large-scale heating rates, **c** longwave and shortwave heating rates, and **d** convective plus large-scale heating rates for various AM2 sensitivity experiments

far clouds can be perturbed in simulations to influence the TOA radiation.

IWP differs significantly among GCM simulations (Waliser et al. 2009). We also note large IWP differences between AM2, HiRAM, and various sensitivity experiments. More specifically, as mentioned above, clouds differ significantly between AM2 and HiRAM, but a TOA radiation balance can still be achieved in both models. It is, thus, revealing to explore the sensitivity of TOA radiation to IWP. Since radiation also depends on other variables (temperature, water vapor, etc.) other than clouds, a comparison of radiation in

these sensitivity experiments cannot isolate the cloud radiative impacts directly. To determine the relative impact of cloud fraction and IWP on TOA radiation, we use offline radiation calculations, which are identical to the radiation code used in model simulations. 3-h model outputs, including cloud fraction, IWC, LWC, temperature, water vapor mixing ratio, surface properties, ozone, and other variables needed for radiation calculation, are fed into the offline radiation kernel. Two groups of idealized calculations are conducted based on 1-year 3-h AM2 simulation outputs. One group is via varying cloud fraction (CF) at model grid points

with  $IWC > 1 \times 10^{-9} \text{ g kg}^{-1}$  and the other group is via the change of IWC at all model grid points. Five CF calculations using (0.98, 0.95, 0.90, 0.80, and 0.50) of AM2 CF, and five IWC calculations using (0.5, 2, 5, 10, 20) times of AM2 IWC are conducted. Though these are idealized calculations, they still provide heuristic guidance for model development, especially regarding tuning clouds to achieve the TOA radiation balance within the measurement uncertainties.

Figure 8 shows the global mean TOA SW absorbed (SWABS) and OLR from these calculations and various RAS sensitivity experiments, with CERES-EBAF (Loeb et al. 2009) values assuming a  $5 \text{ W m}^{-2}$  uncertainty as a reference. In general, both OLR and SWABS decrease with increasing IWC with a strong compensation between SW and LW with a resultant small net imbalance ( $< 4 \text{ W m}^{-2}$ ). This may be part of the reason why IWP can vary significantly in GCMs, but still maintaining a reasonable TOA radiation balance (Waliser et al. 2009). Both OLR and SWABS increase linearly with decreasing CF with a  $\sim 2 \text{ W m}^{-2}$  global TOA net radiative forcing for the CF calculations considered here. These calculations suggest that there are a number of possible combinations of cloud fraction and IWC to achieve a realistic TOA radiation balance in the model considering the satellite measurement uncertainties. For example, AM2 can achieve a realistic TOA radiation with IWC increased by up to five times combined with a 50% reduction of ice cloud fraction. This suggests that clouds simulated in current GCMs have a wide range of uncertainties and compensating errors, which need to be better constrained using better satellite measurements in the future. This analysis reveals the limitation to constrain model TOA radiation only and

highlights the importance, in the future, of constraining model cloud fields and properties using available observations. The other point to note in Fig. 8 is that the LW changes are generally much smaller than SW changes in various RAS sensitivity experiments, especially for RAS-TK experiments. For example, OLR from the three TK experiments barely changes from AM2, though IWP increases significantly (Fig. 8). The reason is that the increased trapping of longwave by larger IWP is partially compensated by the lower temperature and reduced moisture in the upper troposphere as noted above (Fig. 6). One interesting point to note is that the SWABS decrease with increasing IWC in the offline radiation calculations is much larger than that in the TK runs. For example, IWC in RAS-TK8 is  $\sim 10$  times of that in AM2 (Fig. 5a), but the SWABS is only reduced by  $\sim 8 \text{ W m}^{-2}$  from AM2. In contrast, the SWABS is reduced by more than  $\sim 15 \text{ W m}^{-2}$  from AM2 when IWC is increased by ten times in the offline calculation (Fig. 8). The reason is because IWC increase in the RAS-TK8 run is not necessarily at noon time with the largest solar radiation as in AM2, which tends to have maximum convective activity at noon. This suggests that the model not only needs to capture the mean cloud fraction and condensate well, but also needs to have their diurnal variations correctly. In this sense, stand-alone radiation calculation, thus, provides a neat way to narrow down various causal links between cloud and radiation, and will be a useful tool for cloud radiative impact estimates.

## 5 Summary

Cumulus parameterization impacts various aspects of a GCM. IWP and stratiform precipitation fraction over the Tropics differ significantly between GFDL AM2 and HiRAM, which was found to be mainly due to the replacement of RAS in AM2 by the UW scheme. Compared with the active RAS scheme used in AM2, the UW scheme effectively inhibits convection vertical development with a much larger entrainment rate. Consequently, large-scale condensation becomes more active in the upper troposphere and increases the stratiform precipitation and condensate.

Considering the large impact of entrainment specification in cumulus parameterization on model precipitation and cloud, a series of sensitivity experiments based on RAS are conducted to understand their impact on the model tropical cloud and precipitation characteristics. We also conducted several experiments with varying precipitation efficiency and entrainment limiter constant used in RAS significantly modulate model stratiform precipitation fraction, clouds, and TOA radiation over the Tropics. With reduced PE, more convective condensate is left in the air with increased stratiform

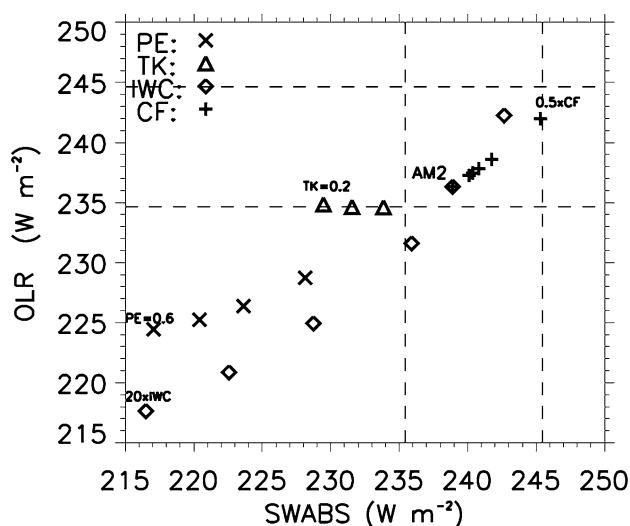


**Fig. 8** a Global TOA OLR and shortwave absorbed (SWABS) from various offline radiation calculations and RAS sensitivity simulations. The dashed lines indicate the CERES-EBAF observations (Loeb et al. 2009) assuming an uncertainty of  $5 \text{ W m}^{-2}$

condensate and cloudiness. This, in turn, affects the radiative heating and atmospheric temperature profile and static stability. The increased static stability reduces convective activity. Increased IWP in reduced PE runs is mainly from the increased detrainment from convection with a minor contribution from reduced convective activity. In contrast, by increasing the Tokioka limiter constant, more deep convection is inhibited. As a result, stratiform heating and precipitation increase, and so do stratiform IWP and cloudiness. Overall, convective and stratiform heating complement each other to help maintain the near moist adiabatic temperature profile over the deep Tropics. However, stratiform heating cannot reach an altitude as high as convective heating due to the dynamics constraint, especially in a model with a coarse resolution. In general, reduced PE results in a warmer and moister middle and upper troposphere, while inhibited convective occurrence contributes to a colder and drier middle and upper troposphere. In terms of TOA radiation, PE reductions significantly reduce OLR and shortwave absorption, but increases of TK only slightly reduce the shortwave absorption with OLR barely changed.

A series of offline radiation calculations are conducted to quantify the impacts of cloud fraction and IWC on TOA radiation. It is found that TOA radiation balance can be achieved by a variety of combination of IWC and cloud fraction. In addition, the diurnal variation of clouds also impacts TOA radiation. As a result, correct cloud fraction and condensate do not necessarily lead to accurate radiation. The model also needs to capture the clouds at the correct time of day.

Despite their importance, cumulus microphysics and entrainment and detrainment are difficult to evaluate and constrain directly by the current observations. Considering their significant and relative straightforward impact on tropical precipitation and cloud, current satellite observations might provide an effective and alternative way to constrain cumulus PE and entrainment indirectly. For example, recent TRMM precipitation retrieval not only provides precipitation intensity distribution, but also the stratiform precipitation fraction. CloudSat gives the first available global IWC distribution and some estimate of precipitation frequency. Atmospheric Radiation Measurement (ARM, Ackerman and Stokes 2003) program has collected extensive cloud, surface precipitation, and radiation at several locations from the Tropics to the polar region. Combined with TOA radiation measurements from satellites, such data set (e.g., Climate Model Best Estimate, Xie et al. 2010) will provide an unprecedented opportunity for cumulus parameterization evaluation and improvement.

**Acknowledgements** The author would like to thank Dr. Ming Zhao at GFDL for various discussions. This work was supported by Tsinghua University Initiative Scientific Research Program (2019Z07L01001).

## References

- Ackerman TP, Stokes GM (2003) The atmospheric radiation measurement program. *Phys Today* 56:38–45
- Adler RF et al (2003) The Version-2 global precipitation climatology project (GPCP) monthly precipitation analysis (1979–present). *J Hydrometeorol* 4:1147–1167
- Anderson et al (2004) The new GFDL global atmosphere and land model AM2-LM2: evaluation with prescribed SST simulations. *J Clim* 17:4641–4673
- Arakawa A (2004) The cumulus parameterization problem: past, present, and future. *J Clim* 17:2493–2525
- Bechtold P, Köhler M, Jung T, Doblas-Reyes F, Leutbecher M, Rodwell M, Vitart F, Balsamo G (2008) Advances in simulating atmospheric variability with the ECMWF model: from synoptic to decadal time-scales. *Q J R Meteorol Soc* 134:1337–1351
- Bretherton CS, McCaa JR, Grenier H (2004) A new parameterization for shallow cumulus convection and its application to marine subtropical cloud-topped boundary layers. Part I: description and 1D results. *Mon Weather Rev* 132:864–882
- Chikira Minoru, Sugiyama Masahiro (2010) A cumulus parameterization with state-dependent entrainment rate. Part I: description and sensitivity to temperature and humidity profiles. *J Atmos Sci* 67:2171–2193
- Clement AC, Soden B (2005) The sensitivity of the tropical-mean radiation budget. *J Clim* 18:3189–3203
- Dai A (2006) Precipitation characteristics in eighteen coupled climate models. *J Clim* 19:4605–4630
- de Rooy WC, Pier Siebesma A (2010) Analytical expressions for entrainment and detrainment in cumulus convection. *Q J R Meteorol Soc* 136:1216–1227. <https://doi.org/10.1002/qj.640>
- Del Genio AD, Kovari W, Yao M-S, Jonas J (2005) Cumulus microphysics and climate sensitivity. *J Clim* 18:2376–2387
- Donner LJ, Seman CJ, Hemler RS, Fan S (2001) A cumulus parameterization including mass fluxes, convective vertical velocities, and mesoscale effects: thermodynamic and hydrological aspects in a general circulation model. *J Clim* 14:3444–3463
- Donner Leo J et al (2011) The dynamical core, physical parameterizations, and basic simulation characteristics of the atmospheric component AM3 of the GFDL global coupled model CM3. *J Clim* 24:3484–3519
- Ehsan MA, Almazroui M, Yousef A (2017a) Impact of different cumulus parameterization schemes in SAUDI-KAU AGCM. *Earth Syst Environ* 1:3. <https://doi.org/10.1007/s41748-017-0003-0>
- Ehsan MA, Almazroui M, Yousef A, Enda O, Tippett MK, Kucharski F, Alkhalaf AA (2017b) Sensitivity of AGCM-simulated regional JJAS precipitation to different convective parameterization schemes. *Int J Climatol* 37:4594–4609. <https://doi.org/10.1002/joc.5108>
- Elsaesser Gregory S, Kummerow Christian D, L'Ecuyer Tristan S, Takayabu Yukari N, Shige Shoichi (2010) Observed self-similarity of precipitation regimes over the tropical oceans. *J Clim* 23:2686–2698
- Emanuel KA, Zivkovic-Rothman M (1999) Development and evaluation of a convection scheme for use in climate models. *J Atmos Sci* 56:1766–1782
- Fowler Laura D, Randall David A (2002) Interactions between cloud microphysics and cumulus convection in a general circulation model. *J Atmos Sci* 59:3074–3098
- Fowler LD, Randall DA, Rutledge SA (1996) Liquid and ice cloud microphysics in the CSU general circulation model. Part I: model description and simulated microphysical processes. *J Clim* 9:489–529
- Fu Q, Liou KN (1993) Parameterization of the radiative properties of cirrus clouds. *J Atmos Sci* 50:2008–2025

- Held IM, Zhao M, Wyman B (2007) Dynamic radiative–convective equilibria using GCM column physics. *J Atmos Sci* 64:228–238
- Houze RA Jr (2004) Mesoscale convective systems. *Rev Geophys* 42:43
- Huffman GJ et al (2007) The TRMM multisatellite precipitation analysis (TMPA): Quasi-global, multiyear, combined-sensor precipitation estimates at fine scales. *J Hydrometeor* 8:38–55
- Kikuchi K, Wang B (2008) Diurnal precipitation regimes in the global tropics. *J Clim* 21:2680–2696
- Kiladis GN, Wheeler MC, Haertel PT, Straub KH, Roundy PE (2009) Convectively coupled equatorial waves. *Rev Geophys* 47:RG2003. <https://doi.org/10.1029/2008rg000266>
- Klein SA, Zhang Y, Zelinka MD, Pincus R, Boyle J, Gleckler PJ (2013) Are climate model simulations of clouds improving? An evaluation using the ISCCP simulator. *J Geophys Res Atmos* 118:1329–1342. <https://doi.org/10.1002/jgrd.50141>
- Kubar TL, Hartmann DL (2008) Vertical structure of tropical oceanic convective clouds and its relation to precipitation. *Geophys Res Lett* 35:L03804. <https://doi.org/10.1029/2007GL032811>
- Kummerow C, Hong Y, Olson WS, Yang S, Adler RF, McCollum J, Ferraro R, Petty G, Shin DB, Wilheit TT (2001) The evolution of the Goddard profiling algorithm (GPROF) for rainfall estimation from passive microwave sensors. *J Appl Meteor* 40:1801–1840
- Li J-LF et al (2012) An observationally based evaluation of cloud ice water in CMIP3 and CMIP5 GCMs and contemporary reanalyses using contemporary satellite data. *J Geophys Res* 117:D16105. <https://doi.org/10.1029/2012JD017640>
- Lin J, Mapes BE, Zhang M, Newman M (2004) Stratiform precipitation, vertical heating profiles, and the Madden–Julian oscillation. *J Atmos Sci* 61:296–309
- Lin Y, Donner LJ, Petch J, Bechtold P, Boyle J, Klein SA, Komori T, Wapler K, Willett M, Xie X, Zhao M, Xie S, McFarlane SA, Schumacher C (2012) TWP-ICE global atmospheric model inter-comparison: convection responsiveness and resolution impact. *J Geophys Res Atmos* 117:D09111
- Lin Y, Zhao Ming, Ming Yi, Golaz Jean-Christophe, Donner Leo J, Klein Stephen A, Ramaswamy V, Xie Shaoheng (2013) precipitation partitioning, tropical clouds, and intraseasonal variability in GFDL AM2. *J Clim* 26:5453–5466
- Loeb NG, Wielicki BA, Doelling DR, Smith GL, Keyes DF, Kato S, Manalo-Smith N, Wong T (2009) Toward optimal closure of the Earth’s top-of-atmosphere radiation budget. *J Clim* 22:748–766
- Moorthi S, Suarez MJ (1992) Relaxed Arakawa–Schubert: a parameterization of moist convection for general circulation models. *Mon Weather Rev* 120:978–1002
- Park S, Bretherton CS, Rasch PJ (2014) Integrating cloud processes in the community atmosphere model, version 5. *J Clim* 27(18):6821–6856. <https://doi.org/10.1175/JCLI-D-14-00087.1>
- Rotstaysn LD (1997) A physically based scheme for the treatment of stratiform clouds and precipitation in large-scale models. I: description and evaluation of the microphysical processes. *Q J R Meteorol Soc* 123:1227–1282
- Sanderson BM, Piani C, Ingram WJ, Stone DA, Allen MR (2008) Towards constraining climate sensitivity by linear analysis of feedback patterns in thousands of perturbed-physics GCM simulations. *Clim Dyn* 30:175–190
- Shimpo Akihiko, Kanamitsu Masao, Iacobellis Sam F, Hong Song-You (2008) Comparison of four cloud schemes in simulating the seasonal mean field forced by the observed sea surface temperature. *Mon Weather Rev* 136:2557–2575
- Simpson J, Wiggert V (1969) Models of precipitating cumulus towers. *Mon Weather Rev* 97:471–489
- Slingo A (1989) A GCM parameterization for the shortwave radiative properties of water clouds. *J Atmos Sci* 46:1419–1427
- Song X, Zhang GJ (2011) Microphysics parameterization for convective clouds in a global climate model: description and single-column model tests. *J Geophys Res* 116:D02201. <https://doi.org/10.1029/2010JD014833>
- Tiedtke M (1993) Representation of clouds in large-scale models. *Mon Weather Rev* 121:3040–3061
- Tokioka T, Yamazaki K, Kitoh A, Ose T (1988) The equatorial 30–60 day oscillation and the Arakawa–Schubert penetrative cumulus parameterization. *J Meteor Soc Jpn* 66:883–901
- Waliser DE et al (2009) Cloud ice: a climate model challenge with signs and expectations of progress. *J Geophys Res* 114:D00A21. <https://doi.org/10.1029/2008jd010015>
- Webb MJ, Senior C, Bony S, Morcrette J-J (2001) Combining ERBE and ISCCP data to assess clouds in the Hadley Centre, ECMWF, and LMD atmospheric climate models. *Clim Dyn* 17:905–922
- Xie S et al (2010) Clouds and more: ARM climate modeling best estimate data. *Bull Am Meteor Soc* 91:13–20
- Yang GY, Slingo J (2001) The diurnal cycle in the tropics. *Mon Weather Rev* 129:784–801
- Zhang MH et al (2005) Comparing clouds and their seasonal variations in ten atmospheric general circulation models with satellite measurements. *J Geophys Res* 110:D15S02. <https://doi.org/10.1029/2004jd005021>
- Zhao M (2014) An investigation of the connections among convection, clouds, and climate sensitivity in a global climate model. *J Clim* 27:5. <https://doi.org/10.1175/jcli-d-13-00145.1>
- Zhao M, Held IM, Lin S-J, Vecchi GA (2009) Simulations of global hurricane climatology, interannual variability, and response to global warming using a 50-km resolution GCM. *J Clim* 22:6653–6678. <https://doi.org/10.1175/2009JCLI3049.1>
- Zhao M, Golaz JC, Held IM, Ramaswamy V, Lin SJ, Ming Y, Ginoux P, Wyman B, Donner LJ, Paynter D, Guo H (2016) Uncertainty in model climate sensitivity traced to representations of cumulus precipitation microphysics. *J Clim* 1:1. <https://doi.org/10.1175/jcli-d-15-0191.1>